Supplementary Materials for

Distinct regimes of particle and virus abundance explain face mask efficacy for COVID-19

Yafang Cheng[†,*], Nan Ma[*], Christian Witt, Steffen Rapp, Philipp Wild, Meinrat O. Andreae, Ulrich Pöschl, Hang Su[†].

* These authors contributed equally to this work.
† Correspondence to: H.S. (h.su@mpic.de) and Y.C. (yafang.cheng@mpic.de)

This PDF file includes:

Supplementary Text S1 to S6
Figs. S1 to S7
Tables S1 to S7

Supplementary Text

S1. Scenarios in Leung et al. (2020)

Leung et al. (2020) reported an average of 5 to 17 coughs during the 30-min exhaled breath collection for virus-infected participants (*10*). Taking the particle size distribution given in Fig. 2, we calculate that one person can emit a total number of 9.31e5 to 2.72e6 particles in a 30 min sampling period. Note that particles > 100 μm were not considered here, and the volume concentrations of particles in the "droplet" mode (2.44e-4 mL, with 4.29e-5 to 2.45e-3 mL in 5% to 95% confidence level) overwhelm those in the "aerosol" mode (7.68e-7 mL, with 3.37e-7 to 5.24e-6 mL in 5% to 95% confidence level).

S2. Virus concentration in Leung et al. (2020)

Many samples in Leung et al. (2020) return a virus load signal below the detection limit (*10*). Thus we adopted an alternative approach, using the statistical distribution, i.e., percentage of positive cases, to calculate the virus concentration. Assuming that samples containing more than 2 viruses (Leung et al., 2020 used $10^{0.3}$# as undetectable values in their statistical analysis) can be detected and the virus number in the samples follows a Poisson distribution, the fraction of positive samples (containing at least 3 viruses) can be calculated with pre-assumed virus concentration per particle volume. The Poisson distribution of viruses in emitted droplets is supported by early experiments, where the amount of bioaerosols or compounds delivered in particles is proportional to its concentration in the bulk fluid used to generate particles, and it is independent of investigated particulate type (fluorescent bead, bacteria or spore) (*19*).

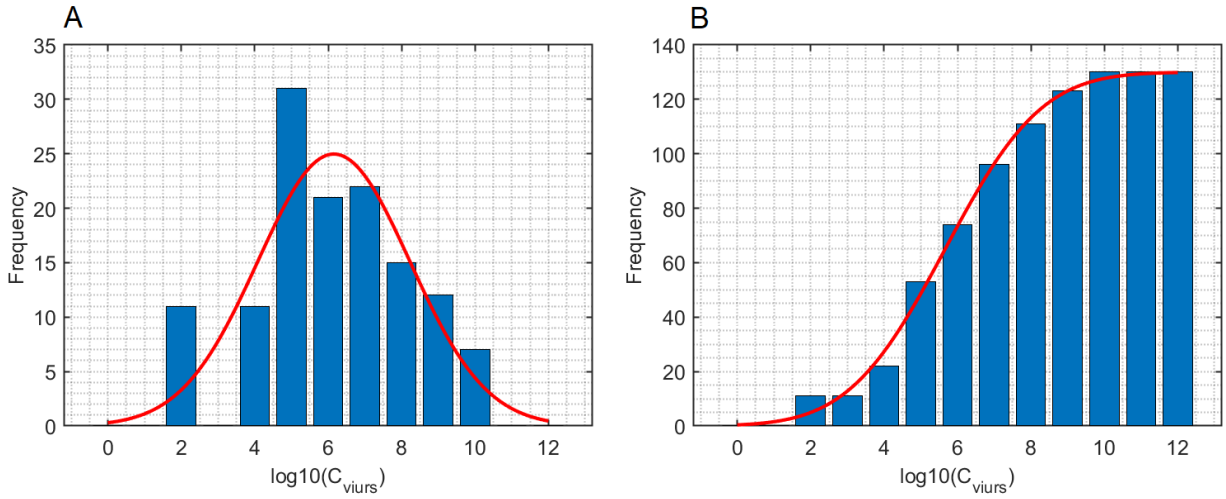

Fig. S1. Statistical distribution of SARS-CoV-2 concentration in sputum samples. (A) Frequency distribution of SARS-CoV-2 concentration. (B) Cumulative distribution of SARS-CoV-2 concentration. The blue bars represent the measured data by Wölfel et al. (2020) (*21*). The red lines show the fit results with a normal distribution function (A) and an error function (B), respectively.

For a set of sufficient samples, the percentage of samples with virus number N >2 (positive samples) is a function of the mathematical expectation of virus number per sample (N_{me}). The N_{me} therefore can be retrieved by scanning a series of N_{me} until the calculated percentage of positive cases agrees with the measurements. It should be noted that the virus concentration in exhaled liquids and the total exhaled liquid volume may be different among individuals, which must be considered in the calculation of virus concentration. Therefore, a Monte Carlo approach is used in this study. We assume that the statistical number distribution of SARS-CoV-2 in sputum samples (Fig. S1, Wölfel et al., 2020) (*21*) can represent the individual difference of virus concentration in exhaled liquids. The distribution can be fitted with a lognormal distribution function with a σ of 2.07. In the experiment of Leung et al. (2020), the difference of sampled liquid volume stems from the individual difference of coughing times and volume concentration of exhaled droplets. The coughing time is assumed to follow a normal distribution with a σ of 44.5. The exhaled droplet volume concentration is assumed to follow a lognormal distribution with a σ of $\log_{10}(2)$. The experiment in Leung et al. (2020) is simulated with a series of virus concentrations. At each virus concentration, the experiment with the same sample number as in Leung et al. (2020) is repeated for 1e5 times to obtain a stable result. For each sample, the mathematical expectation of virus number is calculated based on randomly generated virus concentration, coughing time, and exhaled droplet volume concentration. The "true virus number" in the sample is randomly generated based on Poisson distribution and the calculated mathematical expectation. Finally, for each pre-defined virus concentration, a distribution of positive rates can be obtained and fitted with a normal distribution function. By comparing the simulated positive rates and the reported values in Leung et al. (2020), the concentrations of coronavirus, influenza virus and rhinovirus in exhaled droplets are retrieved (Table S1). And the distribution and median of virus number per sample are calculated (Fig. S2 and Table S2).

Table S1. Virus concentration per particle volume in the exhaled air samples (# mL^{-1}). The concentrations of coronavirus, influenza virus and rhinovirus in aerosol mode (D_w < 5 μm) and droplet mode (D_w > 5 μm) are retrieved based on the measured positive rates of 30-min exhalation samples (*10*). The individual differences of virus concentration and particle emission rate are considered in the calculation.

	Coronavirus	Influenza virus	Rhinovirus
D_w < 5 μm *	5.61e5	4.04e5	3.47e6
D_w > 5 μm *	4.91e2	2.10e2	4.30e2

* During the sampling of exhaled particles in Leung et al. (2020) (*10*), particles with size above and blow 5 μm are separated very close to the mouth, thus the cut size (5 μm) of those two groups of particles is considered as wet diameter (D_w).

Table S2. Virus number in the exhaled air samples (#). The virus number in samples is calculated from the retrieved virus concentration (Table S1) and total volume of exhaled particles during 30-min sampling.

	Coronavirus	Influenza virus	Rhinovirus
D_w < 5 μm	0.750	0.545	4.68
D_w > 5 μm	0.209	0.0909	0.184

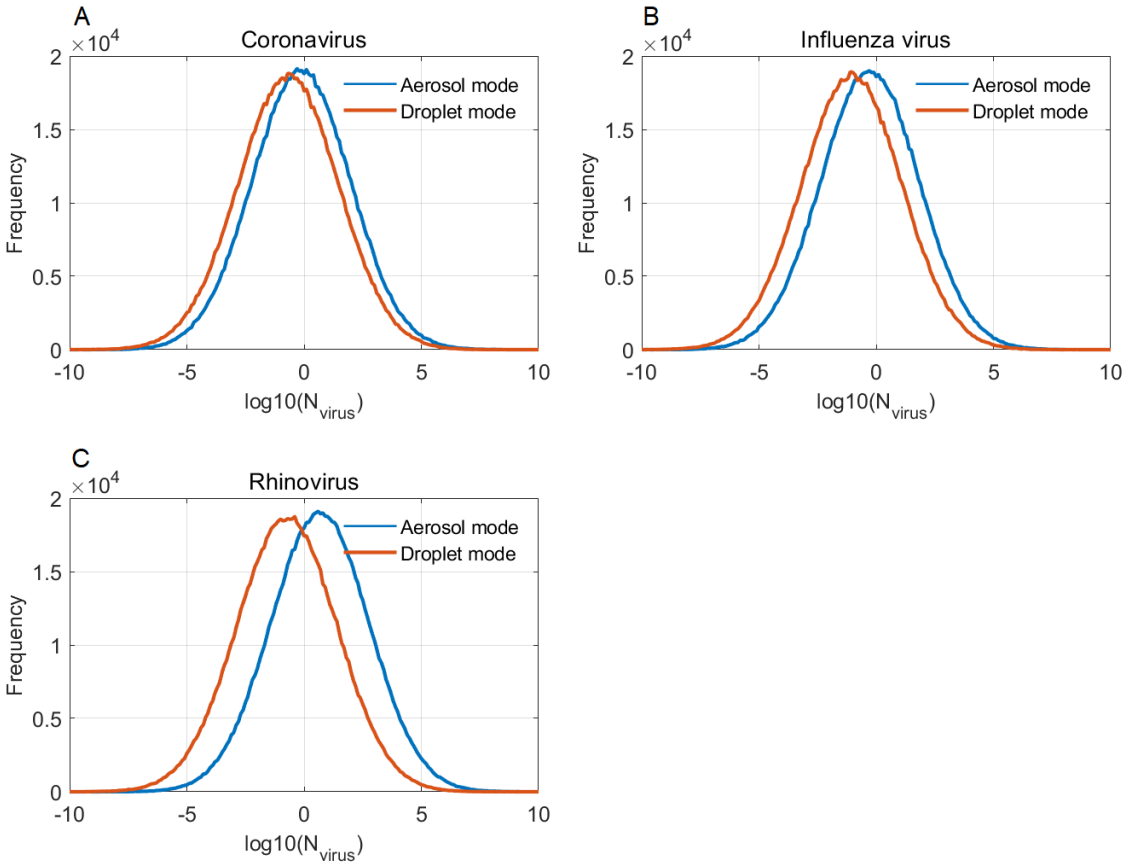

Fig. S2. Frequency distributions of calculated numbers of viruses in 30-min exhaled air samples. (A), (B) and (C) show the distribution of coronavirus, influenza virus and rhinovirus, respectively. In each panel, the blue and red lines represent the virus number in aerosol mode and droplet mode, respectively.

S3. Penetration rate of masks

The size-resolved particle penetration rate of surgical and N95 masks (Fig. S3) is calculated based on the following literature/model calculation:

- Particle diameter < 800 nm: modified from Grinshpun et al. (2009) (*31*)
- Particle diameter > 800 nm & < 5um: modified from Weber et al. (1993) (*32*)
- Particle diameter > 5um: model calculation based on particle impaction with following parameters:
    - Droplets velocity of 6.5 m/s, calculated based on the volume flow rate of 8 L min^{-1} (typical breath flow rate of adults) and an air flow cross section as a circle with a diameter of 1 cm;
    - Impact angle = 90 degree.

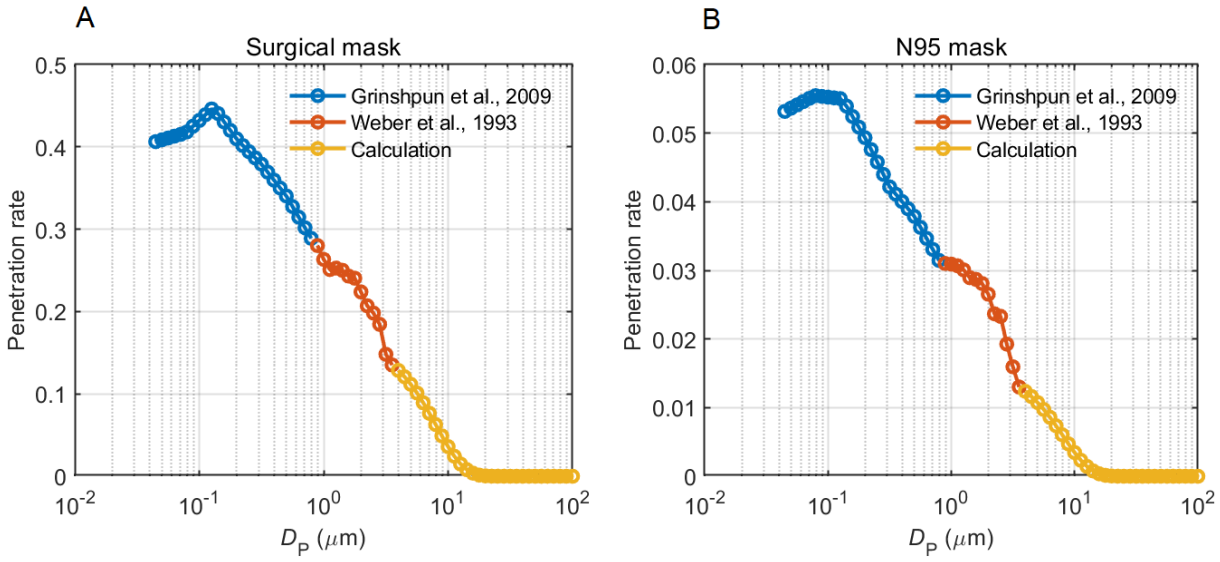

Fig. S3. Particle penetration rate of a surgical mask (A) and a N95 mask (B). For the particle size range of ~50 nm to ~ 800 nm, the penetration rate (blue circle line) is modified from Grinshpun et al. (2009) (*31*). For particle size range of ~800 nm to ~ 3.5 μm, the penetration rate (red circle line) is modified from Weber et al. (1993) (*32*). For particle size above ~3.5 μm, the penetration rate (yellow circle line) is calculated based on particle impaction.

S4. Modelled indoor airborne virus concentrations

To link the results of exhalation samples with ambient samples, we design a scenario with patient density, space areas, and ventilation conditions emulating Fangcang Hospital in Wuhan as follows:

- Each patient coughed an average of 34 times per hour, and the volume of each cough is 2 L; the breath volume is 8 L min^{-1}. The particle size distributions of the coughs and breath were taken from Fig. 2.
- Two cases are assumed:
    - all patients wear surgical masks with penetration rates given in Fig. S3(A), which is the case in Fangcang Hospital (https://edition.cnn.com/2020/02/22/asia/china-coronavirus-roundup-intl-hnk/index.html);
    - all patients do not wear any mask.
- The retrieved concentrations of the three viruses in Sect S2 are used as the virus concentration in exhaled droplets. Same as in Sect S2, the virus concentration is assumed to follow a lognormal distribution with a σ of 2.07, to represent the individual differences.
- The total area of the ward is 500 m^2, the height of the ward is 10 m, and the total number of patients is 200 (*15*).
- Under natural ventilation, the size-resolved loss rate of particles is assumed the same as in Fig. S4 (*33*).
- After being emitted, respiratory particles lose water and dry (to ~ half of the initial particle size) (*34*).

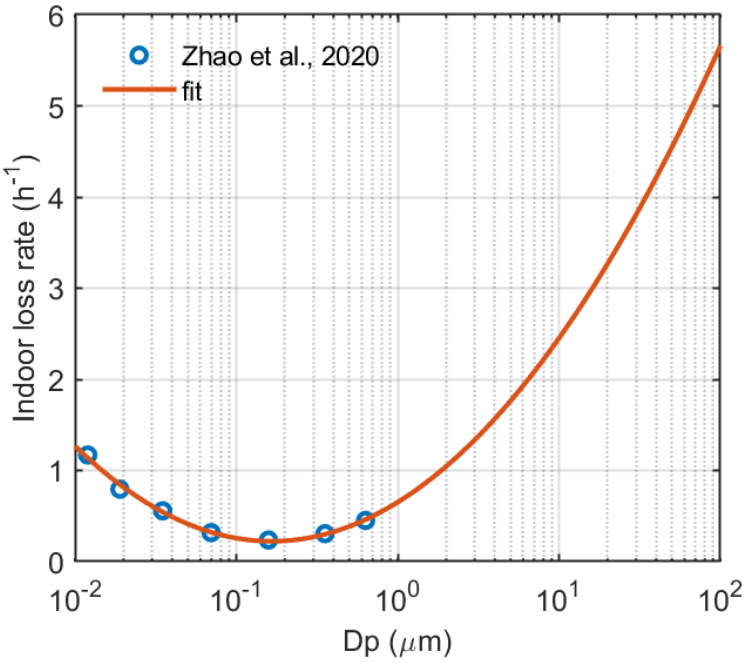

Fig. S4. Size-resolved particle loss rate in indoor environment with natural ventilation. The blue circles represent the measurement in Zhao et al. (2020) (*33*). The red line shows the fit result with $\lambda = 0.703 \cdot D_P^2 + 1.10 \cdot D_P + 0.651$.

When reaching equilibrium in a well-mixed space, the concentration of ambient aerosol particles can be described by:

$$\frac{dn(D_d)}{dt} = \frac{R_E(D_d)}{V} - \lambda(D_d) \cdot n(D_d) = 0 \quad (1)$$

where D_d is the particle dry diameter; n is the number concentration of particles at size bin D_d; R_E is the emission rate of particles by patients; V is the volume of the ward; and λ is particle loss rate due to ventilation and deposition. In the case when all patients were wearing surgical masks,

$$R_E(D_w) = R_{E0}(D_w) \cdot P_{mask}(D_w) \quad (2)$$

where, R_{E0} is the emission rate of patients without wearing mask, D_w is the wet diameter of exhaled droplets, P_{mask} is size-resolved particle penetration rate of surgical masks. In this case, we assumed that exhaled liquid droplets only start to lose water after penetrating masks. In case no patients wearing masks, $R_E(D_w) = R_{E0}(D_w)$. When reaching equilibrium, the ambient particle number size distribution can be calculated as $n = \frac{R_E}{V \cdot \lambda}$. After integration, the volume concentration of particles in the aerosol mode (<2.5 μm, dry state) and droplet mode (>2.5 μm, dry state) can be calculated.

To account for the individual differences of virus concentration in exhaled liquid, a Monte Carlo method is used to get the possible values of airborne virus concentration. The calculation is repeated for 1e7 times with randomly generated in-liquid virus concentrations, which follow a lognormal distribution with a σ of 2.07. The calculated airborne concentrations of coronavirus, influenza virus and rhinovirus are listed in Table S3.

Table S3. Simulated indoor airborne virus concentration in Fangcang Hospital. The indoor airborne concentrations of coronavirus, influenza virus and rhinovirus are simulated for two scenarios: virus emission by patients without wearing surgical masks, and virus emission by patients wearing surgical masks. Median values 5%, and 95% percentiles are given in the table.

Scenarios	Coronavirus (#/m^3) Median (5%, 95%)	Influenza virus (#/m^3) Median (5%, 95%)	Rhinovirus (#/m^3) Median (5%, 95%)
Virus emission/exhalation by patients without wearing surgical masks	0.923 (1.89e-3, 748)	0.514 (1.05e-3, 418)	2.35 (4.66e-3, 2.07e3)
Virus emission/exhalation by patients wearing surgical masks	2.12e-2 (2.67e-5, 36.6)	1.40e-2 (1.65e-5, 25.8)	1.02e-1 (9.75e-5, 218)

Our calculations didn't consider the half-life time of viruses (*35*). With a fixed virus emission rate, the airborne virus concentration is proportional to $\frac{1}{\lambda_v+\lambda_{dep}+k}$, where λ_v, λ_{dep} and k are virus loss rates due to ventilation, deposition and virus inactivation, respectively. The value of k is similar as (or smaller than) λ_v and λ_{dep} (*36*). Therefore, ignoring virus loss due to inactivation (k) has a minor effect on the calculated airborne virus concentrations. The other caveat is that the particle loss rate (λ_v + λ_{dep}) used here may differ from the real loss rate in Fangcang Hospital. According to the loss rate reviewed by Thatcher et al. (2002) (*37*), we may expect a maximum uncertainty of one order of magnitude in the calculated airborne virus concentrations, which will not change the regimes they belong to.

S5. Sample numbers and uncertainties

The test in Leung et al. (2020) is based on 10 samples (*10*). In order to explain the impact of the number of samples and individual difference of virus concentration on the results, a sensitivity experiment is conducted here to simulate the uncertainty of the positive rate of samples obtained under different sample numbers. A Monte Carlo method is applied in the experiment with the following assumptions:

- the number of samples in each experiment is 2, 5, 10, 20, 50, 100, 200, 500 and 1000, respectively;
- the virus concentration in exhaled droplets above and below 5 μm for each person is assumed to follow a lognormal distribution with median value list in Table S1 and a σ of 2.07;
- the actual number of viruses in each sample is randomly determined according to the Poisson distribution based on the calculated mathematical expectations;
- with each sample number, the experiment is repeated for 1e6 times, and the standard deviation (σ) of the derived positive rates is calculated.

The results are shown in Fig. S5. It can be seen that when the number of samples is less than 10, the uncertainty of the observed positive rate is relatively large (σ up to ~0.35). When the number of samples is more than 100, the distribution is narrow, and the uncertainty is small (σ < 0.05).

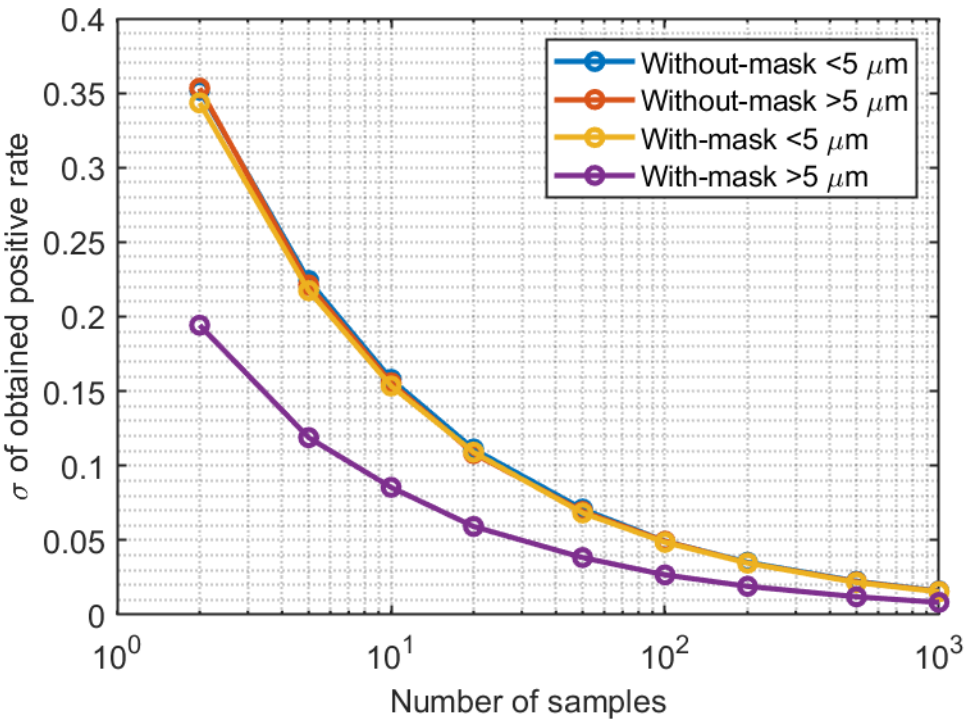

Fig. S5. Standard deviation of positive rates derived based on different sample numbers. Four scenarios are tested: aerosol mode (D_w < 5 μm) samples of 30-min exhalation by patients without wearing surgical masks (blue circle line), droplet mode (D_w > 5 μm) samples of 30-min exhalation by patients without wearing surgical masks (red circle line), aerosol mode (D_w < 5 μm) samples of 30-min exhalation by patients wearing surgical masks (yellow circle line), droplet mode (D_w > 5 μm) samples of 30-min exhalation by patients wearing surgical masks (purple circle line). The virus concentration in exhaled aerosol and droplet mode particles is assumed to be the same as the coronavirus (Table S1).

S6. Effect of wearing masks

We evaluate the effect of wearing masks in controlling the SARS-CoV-2 virus transmission. As detailed below, wearing surgical masks may remove 81% of the SARS-CoV-2 virus. Here, for simplicity, we assume that the percentage change of the virus transmission rate (i.e., the reproductive number) due to airborne transmissions is proportional to the percentage change of transmitted virus numbers. Given a typical reproductive number, R_0, of ~2-3 for COVID-19, wearing a surgical mask can reduce it to ~ 0.47 and thus allow containing the virus. For N95 masks, the reproductive number may even drop to 0.050. This degree of effect is apparently consistent with the real conditions (Fig. S6).

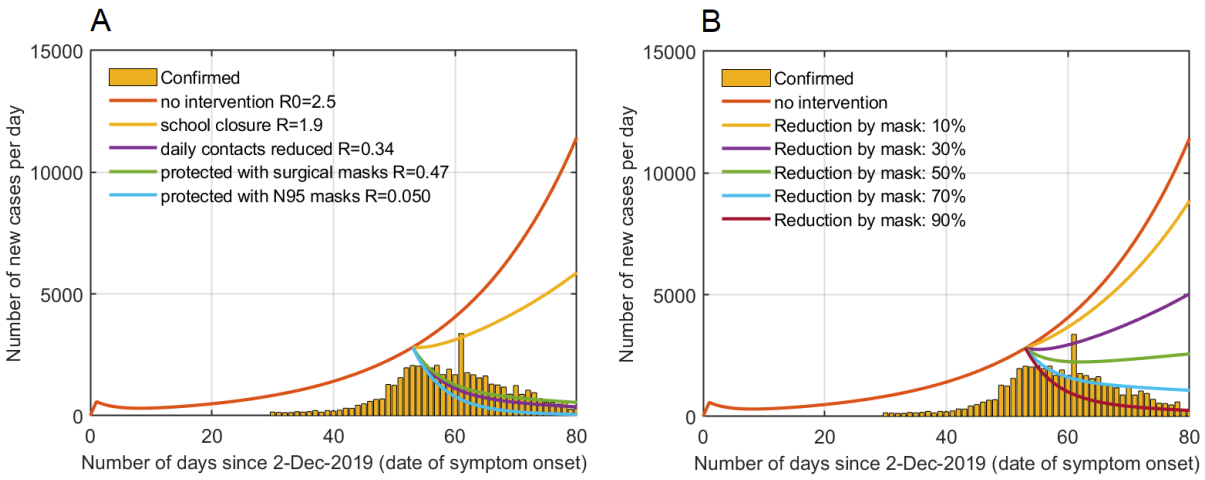

Fig. S6. (A) Reported daily new cases in Wuhan and simulated numbers based on different *R* and control measures. (B) Simulated daily new cases based on different virus emission reduction rates of masks. In panel (A) and (B), the yellow bars represent the confirmed daily new cases in Wuhan and the colored lines show the simulated daily new cases by the SEIR model with different reproduction number *R*.

(1) Effect of wearing masks on reducing the reproduction number *R* of COVID-19

Wearing surgical or N95 masks can reduce the emission rate of virus and further reduce the reproduction number *R* of COVID-19. Assuming that infectious individuals cough on average 20 times and speak for 10 minutes per hour, the emission rate of exhaled droplets ($R_{E,\text{V-drop}}$) can be calculated based on the size distributions shown in Fig. 2, and the emission rate of virus ($R_{E,\text{N-virus}}$) can be calculated with the virus concentration in Table S1. Table S4 shows the results for droplet size range of $D_w < 5$ μm and $D_w < 20$ μm. It can be seen that wearing surgical masks and N95 masks can reduce the emission of virus by 81.4% and 98.0% ($D_w < 20$ μm), respectively.

Assuming that the reproduction number *R* is proportional to the emission rate of virus-containing droplets (*38*), the effect of wearing masks on *R* can be calculated. Assuming a basic reproduction number R_0 of 2.5, all infectious individuals wearing surgical mask and N95 mask can reduce *R* to 0.47 and 0.050, respectively. It should be noted that only the mask removal of virus from the emitters is considered in the calculation. If all people wear masks, the number of viruses inhaled by healthy people will be further reduced, thereby further reduce *R*.

Table S4. Emission rate of droplet volume and virus number by infectious individuals. The emission rates of droplets smaller than 5 μm ($D_w < 5$ μm, $D_d < 2.5$ μm) and smaller than 20 μm ($D_w < 20$ μm, D_d <10 um) are given. Three scenarios, patients without wearing masks, patients wearing surgical masks, and patients wearing N95 mask, are assumed in the calculation.

Scenarios	$D_w < 5$ μm ($D_d < 2.5$ μm)		$D_w < 20$ μm (D_d <10 um)	
	$E_{\text{V-drop}}$ (mL h^{-1})	$E_{\text{N-virus}}$ (h^{-1})	$E_{\text{V-drop}}$ (mL h^{-1})	$E_{\text{N-virus}}$ (h^{-1})
No mask	1.11E-06	6.25E-01	3.27E-05	6.40E-01
Surgical mask	2.11E-07	1.19E-01	1.00E-06	1.19E-01
N95 mask	2.29E-08	1.28E-02	9.88E-08	1.29E-02

(2) The effect of wearing masks on the outbreak and popularity of COVID-19

To evaluate the effect of wearing masks on the dynamics of the COVID-19 outbreak, the infectious disease dynamics model (SEIR model) is employed to model the number of infections (*39*):

$$\begin{cases} \frac{dS_p}{dt} = -\frac{\beta_t S_p I_p}{N_p} \\ \frac{dE_p}{dt} = \frac{\beta_t S_p I_p}{N_p} - \sigma_i E_p \\ \frac{dI_p}{dt} = \sigma_i E_p - \gamma_r I_p \\ \frac{dR_p}{dt} = \gamma_r I_p \\ \beta_t = R_0 \gamma_r \end{cases} \quad (3)$$

where N_p is total population, S_p is the susceptible population, E_p is the exposed population, I_p is infectious population, R_p is recovered or dead population, β_t is the transmission rate, σ_i is the infection rate, γ_r is the recovery rate, and R_0 is the basic reproduction number. Zhang et al. (2020) investigated the effect of limiting social contact patterns on the reproduction number of COVID-19 in Wuhan, China (*40*). We also select Wuhan as the target city, to compare the effects of wearing a mask and limiting social contact patterns reported in Zhang et al. (2020). The parameters in the SEIR model are assumed as follows (*40*, *41*):

- N_p = 11080000;
- γ_r = 0.0556;
- σ_i = 0.1923;
- R_0 = 2.5;
- The first outbreak occurred on December 2, 2019: E_p=3000 and I_p=10.

Assuming that control measures starts on January 24 and no control measures are implemented before January 23, the effects of the following control measures are evaluated with the SEIR model:

- Only school closure: *R*=1.9 (*40*);
- Reduce personnel contact (through home isolation, close public settings, etc.): *R*=0.34 (*40*);
- Wearing surgical masks, no other measures: *R*=0.47;
- Wearing N95 masks, no other measures: *R*=0.050.

Table S5. Total infection number and infection rate in Wuhan calculated based on different *R*. The total infection number and infection rate are simulated with the SEIR model. The *R* for the control measures of school closure (*R*=1.9) and daily contacts reduced (*R*=0.34) are reported in Zhang et al. (2020) (*40*). And the *R* for the control measures of wearing surgical masks (*R*=0.47) and N95 masks (*R*=0.050) are calculated assuming that *R* is proportional to the emission rate of virus-containing droplets.

	R	Total infection number	Total infection rate
No intervention	2.5	9.89E+06	89.3%
School closure	1.9	8.43E+06	76.1%
Daily contacts reduced	0.34	8.69E+04	0.785%
Protected with surgical masks	0.47	1.01E+05	0.915%
Protected with N95 masks	0.050	6.81E+04	0.615%

Figure S6(A) shows the results of the model calculation. Table S5 shows the cumulative total number of infections and the percentage of total infections under the five scenarios. It can be seen that wearing a surgical/N95 mask can reduce the total infection rate to below 1%, which is similar as limiting social contact patterns. And there is no notable difference in reduction of total infection rate between wearing a surgical mask and a N95 mask. As a sensitivity study, we also calculated the total infection number and infection rate based on different virus emission reduction rates of masks. Results are shown in Fig. S6(B) and Table S6.

Table S6. Total infection number and infection rate in Wuhan calculated assuming different virus reduction rates of masks. The total infection number and infection rate are simulated with the SEIR model. The reproduction number *R* is assumed to be proportional to the emission rate of virus-containing droplets.

Reduction rate of mask	*R*	Total infection number	Total infection rate
10%	2.25	9.46E+06	85.4%
30%	1.75	7.91E+06	71.4%
50%	1.25	4.21E+06	38.0%
70%	0.75	1.82E+05	1.65%
90%	0.25	7.94E+04	0.717%

Table S7. Indoor concentration (C_{virus}) and 30-min inhaling number (N_{30}) of SARS-CoV-2 RNA copies in Fangcang Hospital. The table is modified from Liu et al. (2020) (*15*). Room 1 and 2 are Protective Apparel Removal Room, and Room 3 is Medical Staff's Office. In the calculation of N_{30}, the total volume of inhaled air in 30 min is assumed to be 240 L.

	Mode	Room 1	Room 2	Room 3
C_{virus} (# m^{-3})	Aerosol mode (D_{amb} < 2.5 μm) *	41	13	10
	Droplet mode (D_{amb} > 2.5 μm) *	1	7	10
N_{30} (#)	Aerosol mode (D_{amb} < 2.5 μm) *	9.8	3.1	2.4
	Droplet mode (D_{amb} > 2.5 μm) *	0.24	1.7	2.4

* In this study, the aerosol mode and droplet mode are defined as particles with wet diameter (D_w) smaller than 5 μm and lager than 5 μm, respectively. After being emitted, respiratory particles lose water and dry to ~ half of the initial particle size (*34*). Therefore, the boundary of these two modes for ambient particles is at ambient diameter (D_{amb}) of ~2.5 μm.

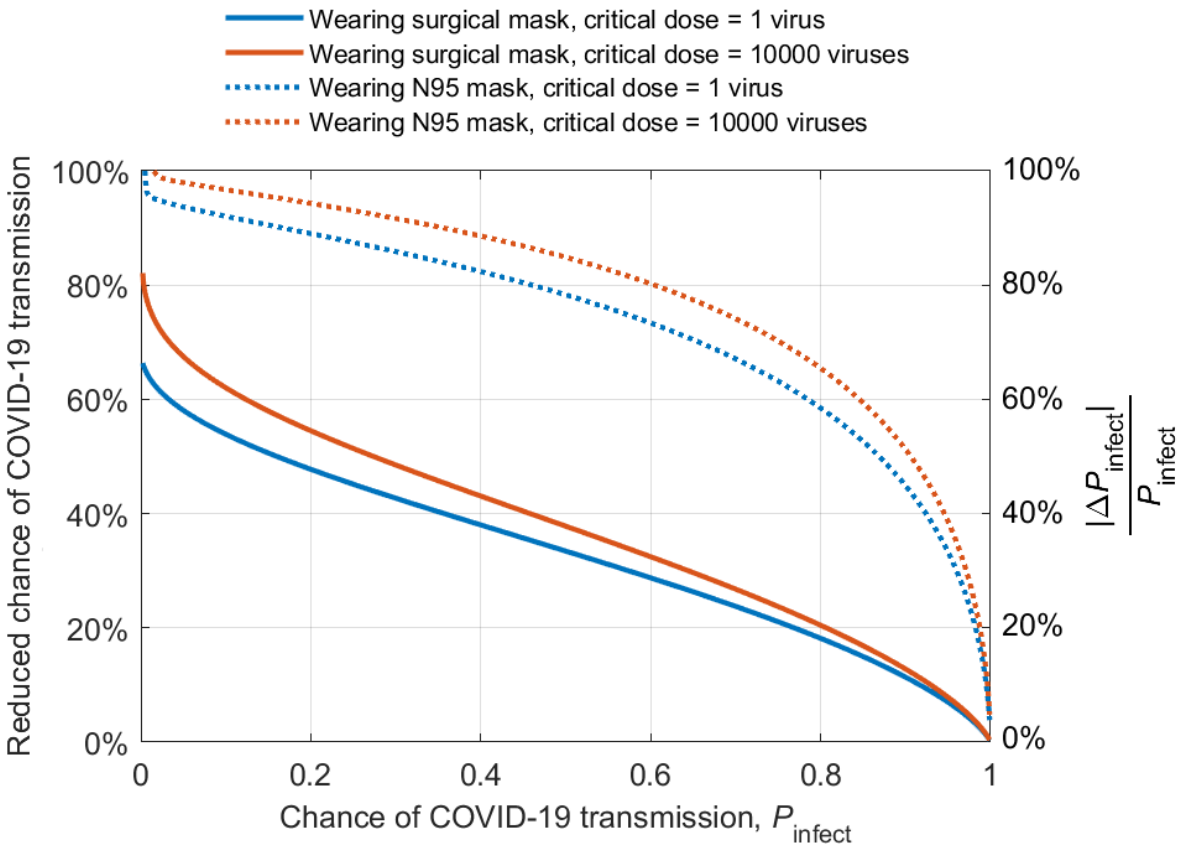

Fig. S7. Reduced chance of COVID-19 transmission with masks. The curves represent the percentage change of P_{infect} caused by mask use due to the change of N_{30}. The blue and red lines represent the results with surgical (blue lines) and N95 masks (red lines) while the solid and dashed lines represent the results for a critical dose of 1 virus and 10000 viruses, respectively. The dependence of P_{infect} on N_{30} used here were assumed the same as in Fig. 3B except that the inhaled virus number is assumed to follow a lognormal distribution with a σ of ~ 1.

References

1. L. Morawska, D. K. Milton, It is Time to Address Airborne Transmission of COVID-19. *Clinical Infectious Diseases*, (2020).
2. S. A. Grinshpun *et al.*, Performance of an N95 Filtering Facepiece Particulate Respirator and a Surgical Mask During Human Breathing: Two Pathways for Particle Penetration. *Journal of Occupational and Environmental Hygiene* **6**, 593-603 (2009).
3. T. Oberg, L. M. Brosseau, Surgical mask filter and fit performance. *American Journal of Infection Control* **36**, 276-282 (2008).
4. T.-C. Hsiao, H.-C. Chuang, S. M. Griffith, S.-J. Chen, L.-H. Young, COVID-19: An Aerosol's Point of View from Expiration to Transmission to Viral-mechanism. *Aerosol and Air Quality Research*, 905-910 (2020).
5. D. K. Chu *et al.*, Physical distancing, face masks, and eye protection to prevent person-to-person transmission of SARS-CoV-2 and COVID-19: a systematic review and meta-analysis. *The Lancet* **395**, 1973-1987 (2020).
6. R. Zhang, Y. Li, A. L. Zhang, Y. Wang, M. J. Molina, Identifying airborne transmission as the dominant route for the spread of COVID-19. *Proc. Natl. Acad. Sci.* **117**, 14857-14863 (2020).
7. C. Y. H. Chao *et al.*, Characterization of expiration air jets and droplet size distributions immediately at the mouth opening. *Journal of aerosol science* **40**, 122-133 (2009).
8. J. P. Duguid, The size and the duration of air-carriage of respiratory droplets and droplet-nuclei. *The Journal of hygiene* **44**, 471-479 (1946).
9. H. Holmgren, E. Ljungström, A.-C. Almstrand, B. Bake, A.-C. Olin, Size distribution of exhaled particles in the range from 0.01 to 2.0μm. *Journal of Aerosol Science* **41**, 439-446 (2010).
10. N. H. L. Leung *et al.*, Respiratory virus shedding in exhaled breath and efficacy of face masks. *Nature Medicine* **26**, 676-680 (2020).
11. K. A. Callow, H. F. Parry, M. Sergeant, D. A. J. Tyrrell, The time course of the immune response to experimental coronavirus infection of man. *Epidemiology and Infection* **105**, 435-446 (1990).
12. T. Watanabe, T. A. Bartrand, M. H. Weir, T. Omura, C. N. Haas, Development of a Dose-Response Model for SARS Coronavirus. *Risk Analysis* **30**, 1129-1138 (2010).
13. A. Roberts *et al.*, Severe Acute Respiratory Syndrome Coronavirus Infection of Golden Syrian Hamsters. *Journal of Virology* **79**, 503-511 (2005).
14. M. Imai *et al.*, Syrian hamsters as a small animal model for SARS-CoV-2 infection and countermeasure development. *Proc. Natl. Acad. Sci.* **117**, 16587-16595 (2020).
15. Y. Liu *et al.*, Aerodynamic analysis of SARS-CoV-2 in two Wuhan hospitals. *Nature* **582**, 557-560 (2020).
16. P. Y. Chia *et al.*, Detection of air and surface contamination by SARS-CoV-2 in hospital rooms of infected patients. *Nat. Commun.* **11**, 2800 (2020).
17. J. L. Santarpia *et al.*, Aerosol and Surface Transmission Potential of SARS-CoV-2. *medRxiv*, 2020.2003.2023.20039446 (2020).
18. J. A. Lednicky *et al.*, Collection of SARS-CoV-2 Virus from the Air of a Clinic within a University Student Health Care Center and Analyses of the Viral Genomic Sequence. *Aerosol and Air Quality Research* **20**, 1167-1171 (2020).

19. M. O. Fernandez *et al.*, Assessing the airborne survival of bacteria in populations of aerosol droplets with a novel technology. *Journal of The Royal Society Interface* **16**, 20180779 (2019).
20. B. Bake, P. Larsson, G. Ljungkvist, E. Ljungström, A. C. Olin, Exhaled particles and small airways. *Respiratory Research* **20**, 8 (2019).
21. R. Wölfel *et al.*, Virological assessment of hospitalized patients with COVID-2019. *Nature* **581**, 465-469 (2020).
22. C. R. MacIntyre *et al.*, Efficacy of face masks and respirators in preventing upper respiratory tract bacterial colonization and co-infection in hospital healthcare workers. *Preventive medicine* **62**, 1-7 (2014).
23. C. R. MacIntyre *et al.*, A randomized clinical trial of three options for N95 respirators and medical masks in health workers. *American journal of respiratory and critical care medicine* **187**, 960-966 (2013).
24. M. Loeb *et al.*, Surgical mask vs N95 respirator for preventing influenza among health care workers: a randomized trial. *Jama* **302**, 1865-1871 (2009).
25. L. J. Radonovich, Jr *et al.*, N95 Respirators vs Medical Masks for Preventing Influenza Among Health Care Personnel: A Randomized Clinical Trial. *Jama* **322**, 824-833 (2019).
26. J. Zhang *et al.*, Changes in contact patterns shape the dynamics of the COVID-19 outbreak in China. *Science* **368**, 1481-1486 (2020).
27. S. Y. Del Valle, J. M. Hyman, H. W. Hethcote, S. G. Eubank, Mixing patterns between age groups in social networks. *Social Networks* **29**, 539-554 (2007).
28. F. M. Guerra *et al.*, The basic reproduction number R_0 of measles: a systematic review. *The Lancet Infectious Diseases* **17**, e420-e428 (2017).
29. W. G. Kreyling, M. Semmler-Behnke, W. Möller, Health implications of nanoparticles. *Journal of Nanoparticle Research* **8**, 543-562 (2006).
30. W. G. Kreyling, M. Semmler-Behnke, W. Möller, Ultrafine particle-lung interactions: does size matter? *Journal of aerosol medicine : the official journal of the International Society for Aerosols in Medicine* **19**, 74-83 (2006).
31. S. A. Grinshpun *et al.*, Performance of an N95 filtering facepiece particulate respirator and a surgical mask during human breathing: two pathways for particle penetration. *Journal of occupational and environmental hygiene* **6**, 593-603 (2009).
32. A. Weber *et al.*, Aerosol penetration and leakae characteristics of masks used in the health care industry. *American Journal of Infection Control* **21**, 167-173 (1993).
33. J. Zhao *et al.*, Particle Mass Concentrations and Number Size Distributions in 40 Homes in Germany: Indoor-to-outdoor Relationships, Diurnal and Seasonal Variation. *Aerosol and Air Quality Research* **20**, 576-589 (2020).
34. M. Nicas, W. W. Nazaroff, A. Hubbard, Toward Understanding the Risk of Secondary Airborne Infection: Emission of Respirable Pathogens. *Journal of Occupational and Environmental Hygiene* **2**, 143-154 (2005).
35. N. van Doremalen *et al.*, Aerosol and Surface Stability of SARS-CoV-2 as Compared with SARS-CoV-1. *New England Journal of Medicine* **382**, 1564-1567 (2020).
36. S. L. Miller *et al.*, Transmission of SARS-CoV-2 by inhalation of respiratory aerosol in the Skagit Valley Chorale superspreading event. *MedRxiv*, (2020).

37. T. L. Thatcher, A. C. K. Lai, R. Moreno-Jackson, R. G. Sextro, W. W. Nazaroff, Effects of room furnishings and air speed on particle deposition rates indoors. *Atmospheric Environment* **36**, 1811-1819 (2002).
38. Y. Drossinos, N. I. Stilianakis, What aerosol physics tells us about airborne pathogen transmission. *Aerosol Science and Technology* **54**, 639-643 (2020).
39. G. Chowell, N. W. Hengartner, C. Castillo-Chavez, P. W. Fenimore, J. M. Hyman, The basic reproductive number of Ebola and the effects of public health measures: the cases of Congo and Uganda. *Journal of Theoretical Biology* **229**, 119-126 (2004).
40. J. Zhang *et al.*, Changes in contact patterns shape the dynamics of the COVID-19 outbreak in China. *Science* **368**, 1481-1486 (2020).
41. H. Wang *et al.*, Phase-adjusted estimation of the number of Coronavirus Disease 2019 cases in Wuhan, China. *Cell Discovery* **6**, 1-8 (2020).